Human Molecular Genetics, 1996, Vol. 5, No. 5 685–691

Heterogeneity in telomere length of human chromosomes

Peter M. Lansdorp[1,2,*], Nico P. Verwoerd[3], Frans M. van de Rijke[3], Visia Dragowska[1], Marie-Térèse Little[1], Roeland W. Dirks[3], Anton K. Raap[3] and Hans J. Tanke[3]

[1]Terry Fox Laboratory, B.C. Cancer Agency, 601 West 10th Avenue, Vancouver, B.C., V5Z 1L3, Canada, [2]Department of Medicine, University of British Columbia, Vancouver, B.C., Canada and [3]Sylvius Laboratory, Department of Cytochemistry and Cytometry, University of Leiden, Wassenaarseweg 72, 2333 Al Leiden, The Netherlands

Received January 15, 1996; Revised and Accepted February 21, 1996

Vertebrate chromosomes terminate in variable numbers of T_2AG_3 nucleotide repeats. In order to study telomere repeats at individual chromosomes, we developed novel, quantitative fluorescence *in situ* hybridization procedures using labeled $(C_3TA_2)_3$ peptide nucleic acid and digital imaging microscopy. Telomere fluorescence intensity values from metaphase chromosomes of cultured human hematopoietic cells decreased with the replication history of the cells, varied up to six-fold within a metaphase, and were similar between sister chromatid telomeres. Surprisingly, telomere fluorescence intensity values within normal adult bone marrow metaphases did not show a normal distribution, suggesting that a minimum number of repeats at each telomere is required and/or maintained during normal hematopoiesis.

INTRODUCTION

Telomeres have important functions in the stability and replication of chromosomes (1,2). These functions are mediated by highly conserved repeats which consist of $(T_2AG_3)_n$ in all vertebrates (3). The number of telomeric repeats in human somatic cells appears to decrease with cell divisions (4–6) and with age (7,8). Telomere shortening may act as a mitotic clock in normal somatic cells (9) and high levels of the enzyme telomerase (capable of elongating telomeres) have been found in tumor cells (10). The most commonly used tool to estimate telomere length is Southern analysis of genomic DNA digested with selected restriction enzymes (11,12). Such analysis requires thousands of cells and provides only a crude estimate (smear) of the average number of T_2AG_3 repeats in the chromosomes of all cells analyzed. In principle, fluorescence *in situ* hybridization (FISH) should be able to provide information on the telomere length of individual chromosomes. Directly labeled oligonucleotide probes are attractive probes for such analysis because of their small size (good penetration properties), single strand nature (no renaturation of probe) and controlled synthesis (13). However, the efficiency of oligonucleotide hybridizations for telomeric repeats has not been sufficient to extend this approach beyond qualitative studies of T_2AG_3 repeat sequences in chromosomes of various species (3,14). Recently, it was shown that synthetic peptide nucleic acid (PNA) oligonucleotide probes will hybridize with complementary oligonucleotide sequences and that the resulting duplexes are more stable than DNA/DNA or DNA/RNA duplexes (15,16). In PNA, the charged phosphate-(dexoxy) ribose backbone of conventional DNA and RNA oligonucleotides is replaced by an uncharged backbone of repeating *N*-(2-amino ethyl)-glycine units linked by peptide bonds. Here we show that the resulting differences in hybridization properties can be exploited for quantitative measurement of repeat sequences by selection of hybridization conditions that allow PNA/DNA hybridization but disfavor renaturation of complementary DNA strands.

RESULTS AND DISCUSSION

In initial studies, we compared directly FITC-labeled DNA, RNA and PNA $(C_3TA_2)_3$ oligonucleotide probes for the detection of T_2AG_3 repeats on human metaphase chromosomes by *in situ* hybridization. At selected hybridization conditions (13) all three probes showed fluorescence of some telomeres (data not shown). Hybridization with the RNA probe appeared somewhat more efficient than with the DNA oligo but neither of these two probes allowed staining of all telomeres in line with previous findings by others (3,13,14). The PNA probe showed a high background fluorescence but also intense staining of most telomeres. Further optimization of the hybridization protocol for use with the PNA probe (see Materials and Methods section) resulted in microscopic images exemplified in Figures 1 and 2.

Essentially all metaphase chromosomes showed four fluorescent spots at telomeric positions (Fig. 1A,C) and up to 92 spots were observed in interphase nuclei (Fig. 1B). This was an unexpected result in view of the failure to visualize all telomeres by regular oligonucleotide hybridization (3,13,14) or the more sensitive primed *in situ* hybridization (17). The telomere fluorescence of sister chromatids appeared of similar intensity (Fig. 1A,C), an impression that was confirmed by image analysis

*To whom correspondence should be addressed

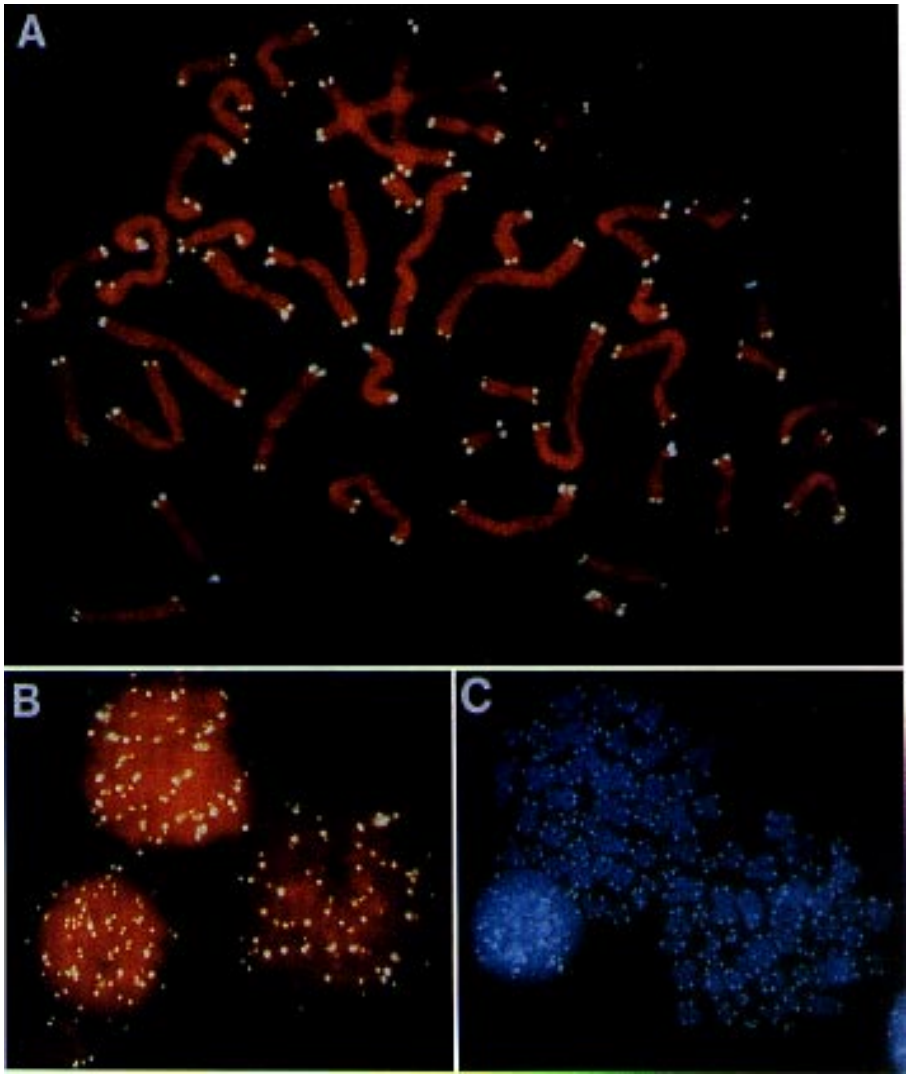

Figure 1. *In situ* hybridization of peptide nucleic acid probe to metaphase chromosomes and interphase nuclei from cultured human fetal liver cells. Conditions for the hybridization of the FITC-labeled $(C_3TA_2)_3$ PNA probe are detailed in the Materials and Methods section. Chromosomes were counterstained with propidium iodide (orange, A&B) or diamidinophenylindole (DAPI, blue, C). Photographs were taken directly from the microscope using a 100× objective. Note that essentially all metaphase chromosomes show four fluorescent spots and that the fluorescence intensity of sister chromatid telomere pairs appears to be linked.

(Fig. 2 and 3). For quantitative purposes digital images from metaphase chromosomes after hybridization with the PNA probe and counter staining with propidium iodide (PI) were captured using a CCD camera (see Materials and Methods section). An example of this type of analysis is shown in Figure 2 and Table 1. Within this individual metaphase, considerable heterogeneity in fluorescence per telomere and in total telomere fluorescence per chromosome was observed. When telomere fluorescence values of all the chromosomes analyzed in this study were analyzed (n = 1273), a good correlation between the values derived from sister chromatid telomere pairs was observed (Fig. 3). Because the members of a sister chromatid telomere pair are expected to contain essentially the same number of T_2AG_3 repeats, this observation suggests that the measured telomere fluorescence intensity values are directly related to the amount of available target sequence (i.e., quantitative hybridization) and that these values are fairly accurate measures of telomere length. Similar correlations between homologous centromere repeat targets were found in earlier quantitative FISH studies (18,19).

Striking differences in the fluorescence intensity of telomeres in cells from fetal liver, adult bone marrow and chronic myeloid leukemia (CML) cells were observed (Figs 4, 5 and Table 2). As shown in Figure 4, the mean telomere fluorescence intensity values (695 for fetal liver, 455 for adult bone marrow and 301 for CML cells) showed a very good correlation with the expected mean terminal restriction fragment (TRF) length for each of these tissues (12 ± 1 kb for fetal liver, 8 ± 1 kb for bone marrow and 5 ± 1 kb for CML cells) (6,20). Several points are worth noting from the data shown in Figure 5. First, independent of the tissue analyzed, telomere fluorescence values varied to a greater extent between chromosomes than was anticipated from the data of flow sorted chromosomes reported by Moyzis (3). Within individual meta-

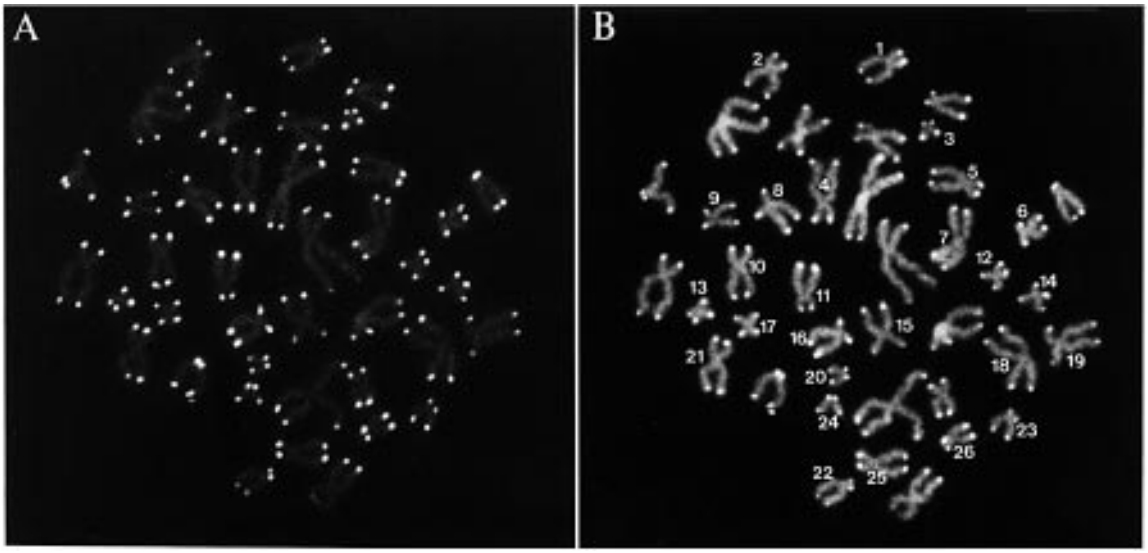

Figure 2. An example of the digital images of *in situ* hybridization of FITC-$(C_3TA_2)_3$ PNA probe to human fetal liver metaphase chromosomes used for calculations of fluorescence intensity of individual telomeres. Microscopic images were captured with a cooled CCD camera (Photometrics) using blue excitation and filters for separate collection of green fluorescence (**A**), mainly FITC; and green plus red fluorescence (**B**), mainly propidium iodide.

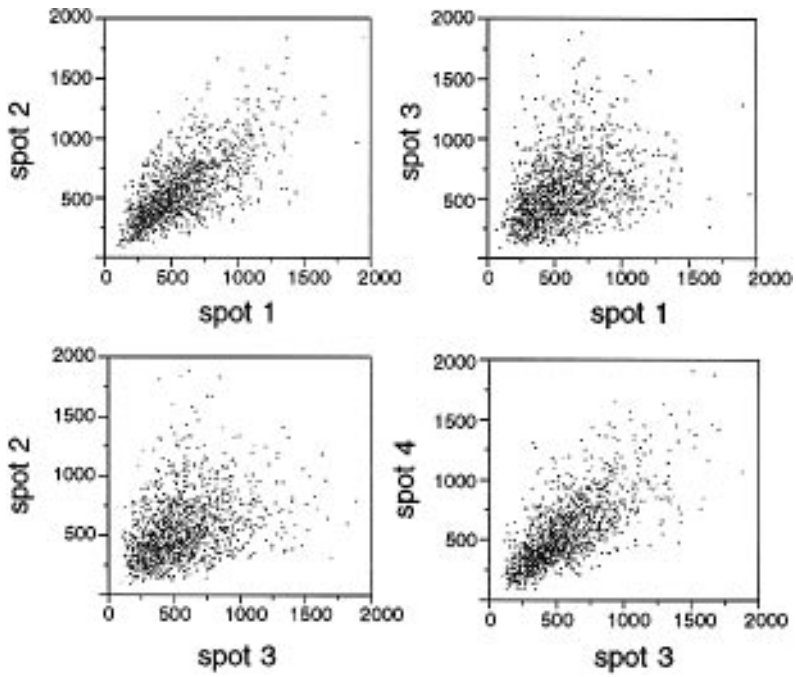

Figure 3. Telomere fluorescence of sister chromatids in metaphase chromosomes is correlated. The fluorescence intensity of individual telomere spots of all the chromosomes analyzed in this study (n = 1273 chromosomes, from cultured fetal liver, cord blood, bone marrow and chronic myeloid leukemia cells) were ranked into two sister chromatid pairs corresponding to their location on each chromosome (i.e. spots 1 and 2 correspond to signals detected on sister chromatids of one arm, while spots 3 and 4 correspond to the two signals on the other arm of the same chromosome). The fluorescence intensity of the individual telomere spots was comparable (mean ± s.d., spot 1: 564 ± 280; spot 2: 562 ± 273; spot 3: 567 ± 288; spot 4: 563 ± 279) but was significantly better correlated between sister chromatid pairs than between telomeres on opposite ends of individual chromosomes (correlation coefficients: spot 1 vs. spot 2 = 0.71; spot 1 vs. spot 3 = 0.35; spot 2 vs. spot 3 = 0.34; spot 3 vs. spot 4 = 0.72; spot 1 vs. spot 4 = 0.33; spot 2 vs. spot 4 = 0.33; spot 1+2 vs. spot 3+4 = 0.39).

phases, the total telomere signal was found to vary around three-fold per chromosome and up to six-fold per telomere (Table 2). The minimum telomere fluorescence values were found to differ less than two-fold between the various tissues. The latter suggests that a threshold or minimum number of T_2AG_3 repeats is required for telomere function. This notion is compatible with studies of telomeres in yeast (1,2) and the observation that immortal tumour cells express high levels of functional telomerase (10). Secondly, the

variation between fluorescence intensity values from different metaphases on the same slide and between slides (BM-1 versus BM-2) appears relatively small (Table 2 and Fig. 5). Together with the observed linkage of sister chromatid telomere fluorescence intensity (Fig. 3), this observation underscores the notion that our PNA-FISH protocol approaches 100% efficiency for the detection of T_2AG_3 repeats. Finally, the distribution of telomere fluorescence appears to be non-random, particularly so in metaphases derived from normal bone marrow and CML cells (Fig. 5). In normal adult bone marrow cells this non-random distribution may be the result of *in vivo* selection of cells that avoided postulated critical telomere shortening (9,21) or, alternatively, a selective action of telomerase on chromosomes with short telomeres. Selection of cells on the basis of telomere shortening would imply that telomeres have an important role in the regulation of normal hematopoiesis in addition to their postulated involvement in cellular senescence (21) and aging (22). Selective action of telomerase on chromosomes with short telomeres (resulting in continuous replication-dependent shortening of long telomeres and the maintenance of short telomeres) is another explanation for the observed skewed distribution of telomere fluorescence intensity values. This hypothesis is compatible with the recent observation that telomerase activity in yeast is negatively regulated by telomere length (23), as well as the presence of measurable telomerase activity in normal bone marrow cells (24–26). A third possibility is that selection of cells as well as selective action of telomerase are jointly responsible for the observed asymmetrical distribution of telomere fluorescence values. Careful analysis of telomere fluorescence from individual chromosomes in clonally propagated normal cells from different tissues using the PNA-FISH technology described here could be used to test these different hypotheses. Such studies are currently in progress. This approach should also reveal whether differences in telomere length are randomly distributed among chromosomes in cells from different tissues.

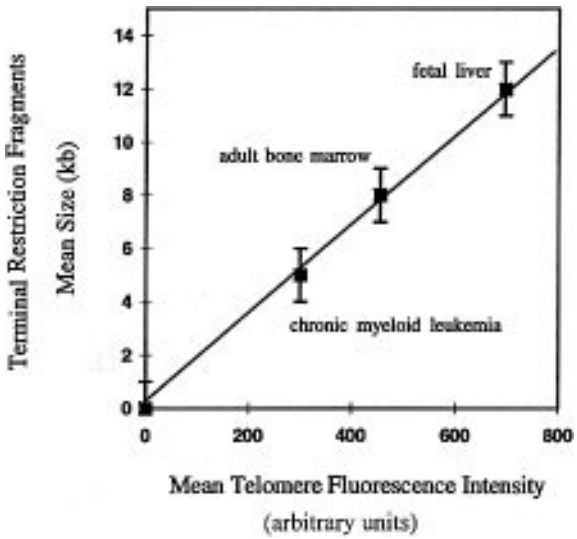

Figure 4. The mean telomere fluorescence intensity (expressed in arbitrary units and measured as described in the Materials and Methods section) is tightly correlated with the mean size of terminal restriction fragments (TRF, expressed in kilobases, kb) obtained by Southern analysis reported for the indicated tissues (6,20). The correlation coefficients between TRF and fluorescence intensity values varied between 0.9 and 0.99 for any TRF value within the indicated range.

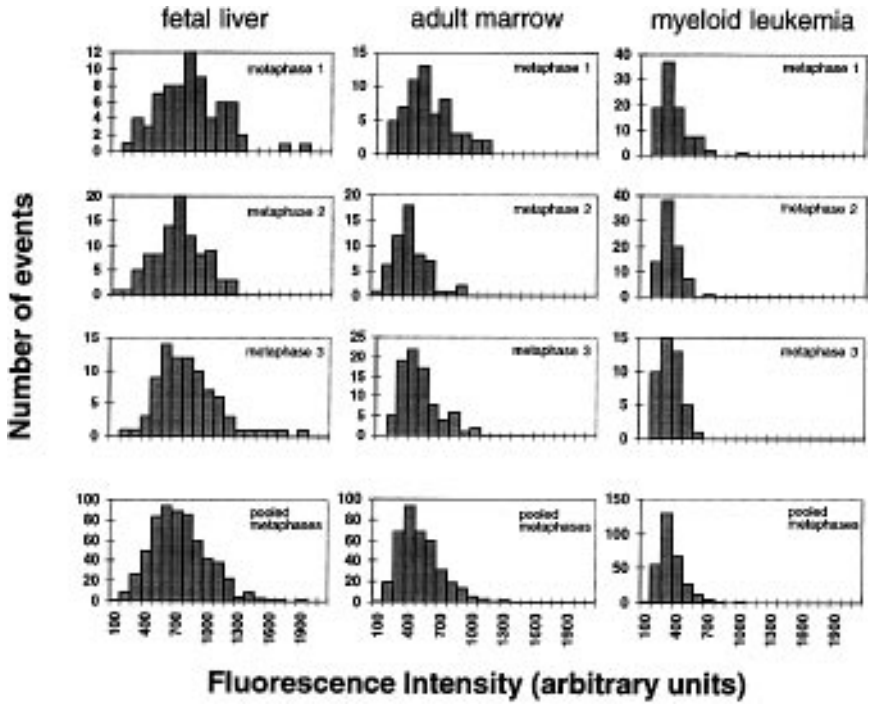

Figure 5. Distribution of telomere fluorescence intensity on metaphase chromosomes from different tissues. Telomere fluorescence (in arbitrary units) was calculated from digital images (as described in the Materials and Methods section). Values for telomere fluorescence (4/chromosome) within the indicated range are shown for three different individual metaphases (numbers corresponding to those in Table 2) as well as the pool of all chromosomes analyzed from each slide/tissue. Note that the distribution of telomere fluorescence within an individual metaphase corresponds well to the overall distribution within the pool of metaphase chromosomes of each tissue and that this distribution is not symmetrical, particularly so in chromosomes of normal adult bone marrow and chronic myeloid leukemia cells.

Table 1. Heterogeneity in telomere fluorescence signals from individual chromosomes of a single metaphase

Chromosome	Pair 1		Pair 2		Sum
no.	Spot 1	Spot 2	Spot 3	Spot 4	
1	698	340	651	622	2311
2	306	334	642	583	1865
3	347	293	727	548	1915
4	546	957	1154	826	3483
5	393	631	609	675	2308
6	478	464	408	581	1931
7	485	431	562	438	1916
8	1071	717	742	923	3453
9	407	357	633	386	1783
10	617	1015	705	657	2994
11	1648	1355	507	372	3882
12	442	483	400	393	1718
13	928	584	383	567	2462
14	712	568	462	359	2101
15	765	529	432	430	2156
16	782	892	1092	964	3730
17	454	307	615	384	1760
18	760	405	689	685	2539
19	398	373	735	521	2027
20	378	405	262	344	1389
21	756	505	774	683	2718
22	312	496	409	407	1624
23	298	359	527	471	1655
24	555	479	456	410	1900
25	641	700	765	475	2581
26	701	774	1085	501	3061

CCD digital images of telomere PNA fluorescence *in situ* hybridization (FISH) on a metaphase spread of a cultured fetal liver cell (shown in Fig. 2 and used for image analysis as described in the Materials and Methods section). The fluorescence intensity of individual telomeres (expressed in arbitrary units) is shown for the 26 chromosomes (arbitrary numbers) indicated in Figure 2. Note the heterogeneity in fluorescence per telomere (i.e., compare data for chromosome 11, spot 1–2 = highest average telomere fluorescence with chromosome 20, spot 3–4 = lowest average telomere fluorescence; ratio 11.1–2/20.3–4 = 5.0) and in the total telomere fluorescence per chromosome (i.e., total fluorescence chr 11/chr 20 = 2.8).

Metaphase preparations from the indicated tissues were hybridized with the PNA-telomere probe and the fluorescence intensity of individual telomeres as well as whole chromosomes (sum of four telomere spots) were measured from digital images as described in the Materials and Methods. The results shown are from individual slides that contained metaphases with at least 10 chromosomes that could be analyzed (i.e. non-overlapping, correct segmentation, four spots). The same fixed bone marrow cells were used to prepare two different slides (BM-1 and BM-2). Min-max values for telomere fluorescence were obtained by averaging the sister chromatid telomere values.

MATERIALS AND METHODS

In situ hybridization

The following hybridization protocol was used to obtain the results shown in the figures and tables of this paper. Cultures of hematopoietic cells from human fetal liver, umbilical cord blood and adult bone marrow were described previously (6). At various time intervals colcemid (0.1 μg/ml) was added to the cultures and cells were harvested 2–18 h later. After washing and hypotonic swelling, cells were fixed and stored in methanol/acetic acid fixative using standard procedures. Cells were fixed to slides by spinning small volumes (10–100 μl) of cells in 2 ml of 50% acetic acid. The slides were dried overnight in air and immersed in Phosphate Buffered Saline (PBS) for 5 min prior to fixation in 4% formaldehyde in PBS for 2 min, washes in PBS (3 × 5 min) and treatment with pepsin (P-7000, Sigma, St. Louis, MO) at 1 mg/ml for 10 min at 37°C at pH 2.0. After a brief rinse in PBS, the formaldehyde fixation and washes were repeated and the slides were dehydrated with ethanol and air dried. Ten microliters of hybridization mixture containing 70% formamide, 0.3 μg/ml FITC-$(C_3TA_2)_3$ PNA probe (PBIO/Biosearch Product, Bedford, MA), 1% (W/V) blocking reagent (Boehringer-Mannheim, Gmbh, FRG) in 10 mM Tris pH 7.2 was added to the slide, a coverslip (20 × 20mm) was added and DNA was denatured by heat for 3 min at 80°C. After hybridization for 2 h at room temperature, the slides were washed at room temperature with 70% formamide/10 mM Tris pH 7.2 (2 × 15 min) and with 0.05 M Tris 0.15 M NaCl pH 7.5 containing 0.05% Tween-20 (3 × 5 min). The slides were then dehydrated with ethanol, air dried and covered by 5–10 μl of antifade solution (VectaShield, Vector

Table 2. Heterogeneity in telomere length on chromosomes from diferent hematopoietic tissues

Tissue	Metaphase	# Chromosomes	Chromosome Values					Telomere Values				
			Min	Max	Ratio	Mean	S.D.	Min	Max	Ratio	Mean	S.D.
FL	1	18	1405	5796	4.12	3101	980	299	1443	4.82	806	264
	2	23	1228	4116	3.35	2603	605	210	1137	5.41	628	198
	3	21	1466	4900	3.34	3050	797	360	1770	4.91	764	253
	4	24	1602	4059	2.53	2861	682	295	1449	4.9	692	226
	5	14	2019	3738	1.85	2971	492	386	1144	2.96	738	167
	6	18	1475	4028	2.73	2735	807	191	1234	6.45	682	224
	7	19	1273	3548	2.78	2224	569	267	978	3.66	542	181
	8	11	2078	4277	2.05	2842	796	349	1117	3.2	716	250
	Pool	**148**	**1568**	**4307**	**2.84**	**2798**	**715**	**294**	**1284**	**4.53**	**695**	**220**
BM-1	1	15	974	3233	3.31	1948	726	166	901	5.43	487	202
	2	14	1015	2463	2.42	1493	431	106	686	6.44	367	141
	3	12	1311	2808	2.14	1727	432	249	943	3.78	431	146
	4	20	1081	2716	2.51	1702	543	221	781	3.53	429	154
	5	18	1083	4019	3.71	2006	708	201	1277	6.36	498	221
	6	16	1540	3007	1.95	1972	407	237	840	5.53	472	128
	Pool	**95**	**1167**	**3041**	**2.67**	**1808**	**541**	**197**	**905**	**4.84**	**449**	**165**
BM-2	1	14	1285	3157	2.45	1958	671	254	992	3.91	467	168
	2	24	1372	3778	2.75	2180	719	209	1074	5.12	522	217
	3	11	1328	2690	2.03	2054	418	263	835	3.17	477	138
	4	14	767	2770	3.61	1822	631	139	942	6.78	456	224
	5	17	1175	3098	2.63	1783	468	219	919	4.19	433	142
	6	13	811	2763	3.41	1921	538	177	712	4.2	465	178
	7	10	874	2915	3.33	1605	697	174	867	4.97	401	221
	Pool	**103**	**1087**	**3024**	**2.88**	**1903**	**591**	**205**	**906**	**4.59**	**460**	**184**
CML	1	23	886	.2144	2.41	1306	350	161	845	5.25	308	128
	2	12	1041	1953	1.88	1391	319	174	769	4.41	343	142
	3	20	943	1872	1.98	1163	229	172	412	2.4	283	69
	4	11	751	1448	1.93	1052	255	157	476	3.03	273	88
	Pool	**66**	**905**	**1854**	**2.05**	**1227**	**288**	**166**	**625**	**3.77**	**301**	**106**

Laboratories Inc., Burlingame, CA) containing 0.1 µg/ml of propidium iodide.

Image analysis

Digital images were recorded with a KAF 1400 slow scan CCD camera (Photometrics; Tuscon, AZ) on an Aristoplan fluorescence microscope (Leica, Wetzlar, Germany), interfaced to a Sun 330 Workstation. Microscope control and image analysis was performed under 'SCIL Image' (TN, Delft; Netherlands). A PL Fluotar 100× NA 1.3 objective lens and a I3 filter block were used for the visualization of FITC and propidium iodide. A short pass SP 560 nm filter was inserted at the emission side when the green FITC emission was recorded, to minimize crosstalk of red propidium iodide signal into this channel. The camera housing contained a short pass SP 630 nm filter to block the far red and infra red light during all measurements. Integration times were chosen such that approximately 50% of the dynamic range of the camera was used (typically 9 s for the FITC telomere signal and 6 s for the propidium iodide counter stain). For these exposure times fading was negligible, due to the anti-fading agent used in the embedding medium. Digital images of 12 bit were corrected for pixel shifts (occurring due to the change of optical filters) by software procedures as described before (27). A second correction procedure was performed to subtract the dark current image and to correct for uneven illumination of the microscopic field and local differences in sensitivity of the camera, using constantly fluorescing uranyl glass as a reference object. Thus recorded and corrected images were segmented on the basis of grey value thresholding to find the contours of the chromosomes and the telomeric regions. For each of the telomeric regions, a background subtraction was performed based on min/max filtering. Each chromosome was divided in four regions by a watershed algorithm, and the integrated fluorescence intensity of each telomeric region was calculated and divided by the integration time used for normalization purposes. Finally, for each chromosome the spot intensities from sister chromatids were ordered two by two and summarized.

ACKNOWLEDGEMENTS

The authors wish to thank Ger van den Engh and Barb Trask (University of Washington, Seattle, WA), Michael Egholm (Biosearch, Bedford, MA), and Connie Eaves (Vancouver, Canada) for advice and stimulating discussions. These studies were supported by NIH grants AI29524 and grant N012104 from the Medical Research Council of Canada. Most of the work described here was performed in the Sylvius Laboratory (Leiden, The Netherlands, supported by NWO grant 900–790–129) during the first half of 1995 by Peter Lansdorp (on sabbatical leave, jointly funded by the B.C. Cancer Agency and the European Cancer Centre with a grant from the Dutch Cancer Society).

REFERENCES

1. Blackburn, E. H. (1994) Telomeres: No end in sight. *Cell*, **77**, 621–623.
2. Sandell, L. L. and Zakian, V.A. (1993) Loss of a yeast telomere: Arrest, recovery and chromosome loss. *Cell*, **75**, 729–739.
3. Moyzis, R. K., Buckingham, J.M., Cram, L.S., Dani, M., Deaven, L.L., Jones, M.D., Meyne, J., Ratliff, R.L. and Wu, J-R. (1988) A highly conserved repetitive DNA sequence, $(TTAGGG)_n$, present at the telomeres of human chromosomes. *Proc. Natl Acad. Sci. USA* **85**, 6622–6626.
4. Allsopp, R. C., Vaziri, H., Patterson, C., Goldstein, S., Younglai, E.V., Futcher, A.B., Greider, C.W. and Harley, C.B. (1992) Telomere length predicts replicative capacity of human fibroblasts. *Proc. Natl Acad. Sci. USA* **89**, 10114–10118.
5. Vaziri, H., Schachter, F., Uchida, I., Wei, L., Zhu, X., Effros, R., Cohen, D. and Harley, C.B. (1993) Loss of telomeric DNA during aging of normal and trisomy 21 human lymphocytes. *Am. J. Hum. Genet.* **52**, 661–667.
6. Vaziri, H., Dragowska, W., Allsopp, R.C., Thomas, T.E., Harley, C.B. and Lansdorp, P.M. (1994) Evidence for a mitotic clock in human hematopoietic stem cells: Loss of telomeric DNA with age. *Proc. Natl Acad. Sci. USA* **91**, 9857–9860.
7. Harley, C. B., Futcher, A.B. and Greider, C.W. (1990) Telomeres shorten during ageing of human fibroblasts. *Nature*, **345**, 458–460.
8. Hastie, N. D., Dempster, M., Dunlop, M.G., Thompson, A.M., Green, D.K. and Allshire, R.C. (1990) Telomere reduction in human colorectal carcinoma and with ageing. *Nature*, **346**, 866–868.
9. Harley, C. B., Vaziri, H., Counter, C.M. and Allsopp, R.C. (1992) The telomere hypothesis of cellular aging. *Exp. Gerontol.* **27**, 375–382.
10. Kim, N. W., Piatyszek, M.A., Prowse, K.R., Harley, C.B., West, M.D., Ho, P.L.C., Coviello, G.M., Wright, W.E., Weinrich, S.L. and Shay, J.W. (1994) Specific association of human telomerase activity with immortal cells and cancer. *Science*, **266**, 2011–2015.
11. Allshire, R. C., Gosden, J.R., Cross, S.H., Cranston, G., Rout, D., Sugawara, N., Szostak, J.W., Fantes, P.A. and Hastie, N.D. (1988) Telomeric repeat from T. thermophila cross-hybridizes with human telomeres. *Nature*, **332**, 656–659.
12. de Lange, T., Shiue, L., Myers, R., Cox, D.R., Naylor, S.L., Killery, A.M. and Varmus, H.E. (1990) Structure and variability of human chromosome ends. *Mol. Cell. Biol.* **10**, 518–527.
13. Meyne, J. and Moyzis, R.K. (1994) *In situ* hybridization using synthetic oligomers as probes for centromere and telomere repeats. *Methods. Mol. Biol.* **33**, 63–74.
14. Meyne, J., Baker, R.J., Hobart, H.H., Hsu, T.C., Ryder, O.A., Ward, O.G., Wiley, J.E., Wurster-Hill, D.H., Yates, T.L. and Moyzis, R.K. (1990) Distribution of non-telomeric sites of the $(TTAGGG)_n$ telomeric sequence in vertebrate chromosomes. *Chromosoma*, **99**, 3–10.
15. Nielsen, P. E., Egholm, M., Berg, R.H. and Buchardt, O. (1991) Sequence-selective recognition of DNA by strand displacement with a thymine-substituted polyamide. *Science*, **254**, 1497–1500.
16. Egholm, M., Buchardt, O., Christensen, L., Behrens, C., Freier, S., Driver, D.A., Berg, R.H., Kim, S.K., Norden, B. and Nielsen, P.E. (1993) PNA hybridizes to complementary oligonucleotides obeying the Watson-Crick hydrogen bonding rules. *Nature*, **365**, 566–568.
17. Therkelsen, A. J., Nielsen, A., Koch, J., Hindkjaer, J. and Kolvraa, S. (1995) Staining of human telomeres with primed in situ labeling (PRINS). *Cytogenet. Cell.Genet.* **68**, 115–118.
18. Nederlof, P. M., van der Flier, S., Raap, A.K. and Tanke, H.J. (1992) Quantification of inter- and intra-nuclear variation of fluorescence *in situ* hybridization signals. *Cytometry*, **13**, 831–838.
19. Celeda, D., Aldinger, K., Haar, F-M., Hausmann, M., Durm, M., Ludwig, H. and Cremer, C. (1994) Rapid fluorescence *in situ* hybridization with repetitive DNA probes: Quantification by digital image analysis. *Cytometry*, **17**, 13–25.
20. Yamada, O., Oshimi, K., Motoji, T. and Mizoguchi, H. (1995) Telomeric DNA in normal and leukemic blood cells. *J. Clin. Invest.* **95**, 1117–1123.
21. Wright, W. E. and Shay, J.W. (1995) Time, telomeres and tumours: is cellular senescence more than an anticancer mechanism? *Trends Cell Biol.* **5**, 293–297.
22. Levy, M. Z., Allsopp, R.C., Futcher, A.B., Greider, C.W. and Harley, C.B. (1992) Telomere end-replication problem and cell aging. *J. Mol. Biol.* **225**, 951–960.
23. McEachern, M. J. and Blackburn, E.H. (1995) Runaway telomere elongation caused by telomerase RNA gene mutations. *Nature*, **376**, 403–409.
24. Broccoli, D., Young, J.W. and de Lange, T. (1995) Telomerase activity in normal and malignant hematopoietic cells. *Proc. Natl Acad. Sci. USA*, **92**, 9082–9086.
25. Hiyama, K., Hirai, Y., Kyoizumi, S., Akiyama, M., Hiyama, E., Piatyszek, M.A., Shay, J.W., Ishioka, S. and Yamakido, M. (1995) Activation of telomerase in human lymphocytes and hematopoietic progenitor cells. *J. Immunol.* **155**, 3711–3715.
26. Chiu, C-P., Dragowska, W., Kim, N.W., Vaziri, H., Yui, J., Thomas, T.E., Harley, C.B. and Lansdorp, P.M. (1996) Differential expression of telomerase activity in hematopoietic progenitors from adult human bone marrow. *Stem Cells*, (in press).
27. Nederlof, P. M., van der Flier, S., Verwoerd, N.P., Vrolijk, J., Raap, A.K. and Tanke, H.J. (1992) Quantification of fluorescence in situ hybridization signals by image cytometry. *Cytometry*, **13**, 846–852.